

## Coupled bunch instability caused by an electron cloud

M. Tobiyama, J. W. Flanagan, H. Fukuma, S. Kurokawa, K. Ohmi, and S. S. Win

*High Energy Accelerator Research Organization (KEK), 1-1 Oho, Tsukuba 305-0801, Japan*

(Received 25 August 2005; published 3 January 2006)

A coupled-bunch instability caused by an electron cloud has been observed in the KEKB LER. The time evolution of the instabilities just after the turning-off the transverse bunch feedback was recorded with several weak solenoid-field conditions, which are used to suppress the vertical blowup of the beam size due to the electron cloud. The mode spectra and their growth rates of the coupled-bunch instabilities were compared with simulations of electrons moving in drift space, a weak solenoid field, and a strong bending field. Mode spectra without a solenoid field support the model where the instability is dominated by the electron clouds in the drift space with a lower secondary yield of photoelectron  $\delta_{2,\max} = 1.0$  rather than 1.5. With the solenoid field, the behavior of unstable modes and the growth rate with the strength of solenoid field also support the simulation with lower secondary emission yield.

DOI: [10.1103/PhysRevSTAB.9.012801](https://doi.org/10.1103/PhysRevSTAB.9.012801)

PACS numbers: 29.27.Bd, 29.20.Dh

### I. INTRODUCTION

In a multibunch positron storage ring with a narrow bunch spacing, electrons created by the synchrotron radiation and the secondary emission due to the absorption of primary electrons at the vacuum chamber surface build up in the vacuum chamber by successive production. An electron cloud with a certain density is formed in the chamber and interacts with the beam that passes through it. The motions of the bunches are correlated with each other if the information of the previous bunch is retained in the cloud. A small betatron oscillation of a bunch is transmitted, amplified to other bunches via the electron cloud, with the result that a coupled-bunch instability is caused.

Transverse coupled-bunch instabilities caused by electron clouds have been observed in many positron storage rings [1–4]. In KEKB LER, we also observed strong transverse coupled-bunch instabilities, and an increase of the vertical beam size. Both of them are believed to be caused by the electron cloud effect [5]. To suppress beam blowup and the coupled-bunch instability, we would weak-solenoid magnets in almost all of the straight sections of the LER ring with a typical magnetic field of 4.5 mT. Currently, the solenoids cover more than 95% of the drift space of KEKB LER. Bunch-by-bunch feedback systems also have been used to suppress any coupled-bunch instabilities [6]. Both systems showed excellent performance to suppress the electron cloud effect, resulting to achieve a very high luminosity of larger than  $1.5 \times 10^{34} \text{ cm}^{-2} \text{ s}^{-1}$  [7].

The bunch-by-bunch feedback systems of KEKB have the function to record the individual bunch motion in 4096 turns (BOR: bunch oscillation recorder) with synchronization to feedback events, such as opening or closing the feedback loop [8]. By analyzing the BOR data obtained just after opening the transverse feedback loop, we can see the clear mode spectrum of the coupled-bunch instabilities, which can then be compared with the model of the insta-

bilities. Early experiment performed at KEKB LER showed that the existence of a solenoid field strongly affects the mode of the coupled-bunch instability [5,9].

In order to study the effect of the solenoid field further, we measured the evolution of the coupled-bunch instabilities at KEKB LER with changing the magnetic field of the solenoid magnets or the length of the drift space covered by the solenoid field. The results were compared with a numerical simulation with electrons moving in drift space, a weak solenoid field and a strong bending field-dominating drift space. The basic parameters of the KEKB LER are given in Table I.

### II. EXPERIMENTAL CONDITIONS

The bunch-filling pattern used in the experiment was a 4-buckets (8 ns) equally spaced pattern with a total number of stored bunch of 1154 bunches, with about 1  $\mu\text{s}$  of empty buckets for the beam-abort system. Figure 1 shows an example of the filling pattern during the experiment. We stored 600 mA ( $0.52 \pm 0.02$  mA/bunch) in LER only, then opened the transverse (either horizontal or vertical) feed-

TABLE I. Basic parameters of the KEKB LER.

Parameter	Symbol	
Energy	$E$	3.5 GeV
Circumference	$L$	3016.26 m
Nominal bunch current	$I_b$	1.3 mA
Nominal bunch spacing	$t_{sp}$	2 ~ 8 ns
Harmonic number	$h$	5120
Rms beam sizes	$\sigma_x$	0.42 mm
	$\sigma_y$	0.06 mm
	$\sigma_z$	7 mm
Betatron tune	$\nu_x/\nu_y$	45.51/43.57
RF voltage	$V_{RF}$	8.0 MV
Synchrotron tune	$\nu_s$	0.024
Radiation damping time	$\tau_x, \tau_y$	40 ms

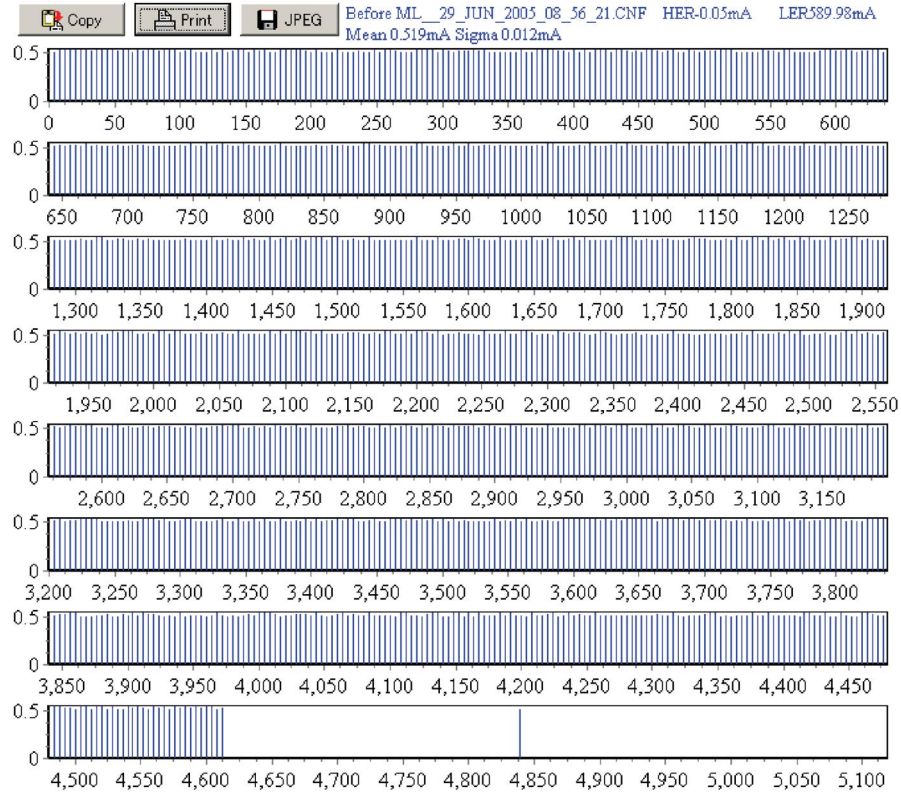


FIG. 1. (Color) Typical filling pattern during experiment.

back loop. We recorded the evolution of the instability during 4096 turns (41 ms) using the BOR, and then closed the loop again to avoid any beam loss. This way to analyze the instability in time-domain is known as transient-domain analysis [10–13]. Because the growth times of the instability in many cases were much shorter than the feedback-off period, typically around 2 ms, recapturing the beam was very difficult.

The conditions of the weak solenoid field in the drift space of the ring of the experiments are given in Table II, where  $B_{\text{sol}}$  means the ratio of the field strength and  $L_{\text{sol}}$  means the ratio of the length covered by the solenoid field relative to normal operating conditions. The change of the conditions of the weak solenoid affects the beam optics, such as the  $x$ - $y$  coupling or dispersion. We therefore performed an optics correction, that is  $x$ - $y$  coupling correction and a dispersion correction both for the horizontal and vertical planes, every time after the change of conditions with a stored current of 30 mA.

TABLE II. Experimental conditions of solenoid field.

Experiments	$B_{\text{sol}}$	$L_{\text{sol}}$
Reference	100%	100%
No solenoid	0%	0%
Effect of $B_{\text{sol}}$	10%, 20%	100%
Effect of $L_{\text{sol}}$	100%	60% or 80%

Since we found that the growth rate of the instability strongly depended on the experimental conditions, especially when we lowered the strength of the solenoid, we tried to moderate the growth rate by increasing the linear chromaticity  $\Delta\xi_{x,y}$ , because it is fairly difficult to analyze the mode of the instability with data of a very short time interval. From a practical view, moderating the very fast growth of the instability during the experiment is very important because it can easily damage both the Belle detector at the collision point and the accelerator components such as radiation masks. We measured the chromaticity  $\xi_{x_0}$  and  $\xi_{y_0}$  on every optics correction. The real chromaticity for the measurement is given as  $\xi_{x,y} = \xi_{x_0,y_0} + \Delta\xi_{x,y}$ . For example, in the case of  $B_{\text{sol}} = 100\%$  with  $L_{\text{sol}} = 100\%$ , the measured linear chromaticities at optics correction were  $\xi_{x_0} = 0.5$ ,  $\xi_{y_0} = 3.8$ . On the horizontal measurement, we increased the horizontal chromaticity by  $\Delta\xi_x = 1$ , therefore the real chromaticity was  $\xi_x = 1.5$ . On the vertical measurement, we tried vertical chromaticity with  $\Delta\xi_y = -2$  or  $\Delta\xi_y = -3$ , therefore the real vertical chromaticity was  $\xi_y = 1.8$  or  $\xi_y = 0.8$ , respectively.

We measured the effect of changes of the chromaticity under several experimental conditions. Figure 2 shows an example of the change of the vertical growth rate with three vertical chromaticities, where the weak solenoid was turned off. By fitting the curve with a linear equation and

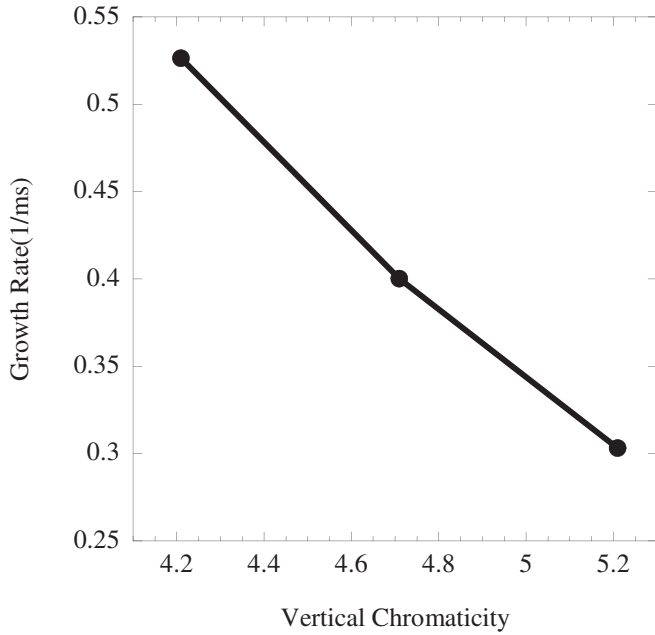


FIG. 2. Example of the change of the vertical growth rate of the instability with changing the vertical linear chromaticity. One point corresponds to one growth experiment. All weak solenoids were set at 0% of field strength.

taking mean of the results under several experimental conditions, we obtained the lowest order effect of the chromaticity as:

- (i) For the horizontal plane:  $-0.105/\text{ms}/\Delta\xi_x$ .
- (ii) For the vertical plane:  $-0.195/\text{ms}/\Delta\xi_y$ .

These results are in good agreement with a theoretical calculation of the head-tail damping effect. The ranges of the chromaticities during the experiment for the horizontal and vertical planes were  $1.08 \sim 9.43$  and  $0.8 \sim 10.64$ , respectively. Since we always used the very beginning of the growth to measure the growth rate, the corresponding

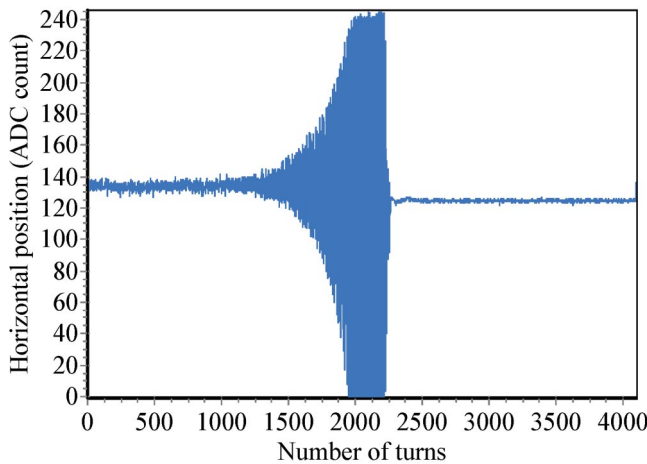


FIG. 3. (Color) Growth of the horizontal oscillation without a solenoid field.

amplitudes of the oscillation for all the measurements were very small.

The position data obtained by the BOR has a bunch-current dependence. We calibrated the data by using the local bump around the beam-position monitor. The result was roughly 0.02 mm/count for the horizontal plane, 0.08 mm/count for the vertical plane with a bunch current of 0.5 mA.

### III. MODE OF THE COUPLED-BUNCH INSTABILITY

#### A. Analysis procedure

We recorded 4096 turns of bunch positions for all 5120 buckets with a 8-bit dynamic range. The unstable modes of the instability were calculated by the following method:

- (i) Make FFT of base 5 for the oscillation data of 256 turns ( $= 5120 \text{ bunches} \times 256 \text{ data points}$ ) to obtain the whole spectrum.
- (ii) Extract amplitude of the spectrum that corresponds to the betatron frequencies ( $f_\beta + m \times f_{\text{rev}}$ ), where  $m$  represents the mode of the oscillation. By aligning the amplitude by increasing order of the mode-id, we obtain the mode spectrum of the instability.
- (iii) Repeat the above procedure while advancing the starting-point of the data by 128 turns. The time evolution of the unstable mode is clearly shown.

Figure 3 shows an example of the growth of a horizontal bunch oscillation from just after opening the horizontal feedback loop to 4096 turns of revolution ( $\sim 41 \text{ ms}$ ), where all of the solenoids were turned off. By making the FFT on this bunch, we found a betatron frequency of 46.59 kHz (52.8 kHz), which corresponds to 0.53 in fractional betatron tune. Because the growth was too fast, the beam was lost after about 2300 turns. With the mode analysis described above, we obtained the time evolution of the unstable modes, as shown in Fig. 4. Since the bunch-

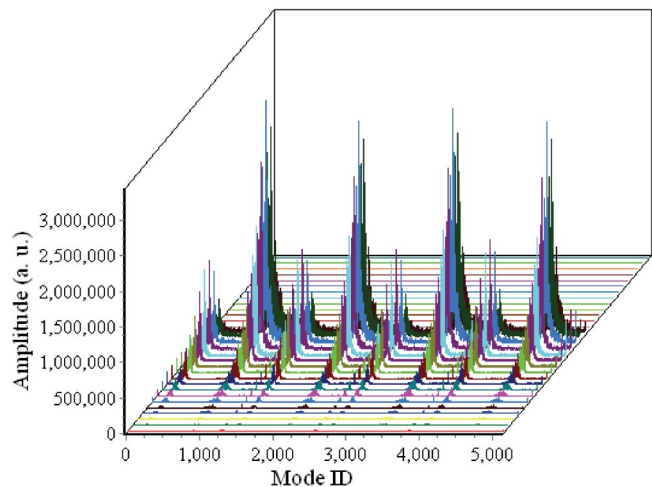


FIG. 4. (Color) Time evolution of the horizontal unstable modes when all the solenoids were turned off.

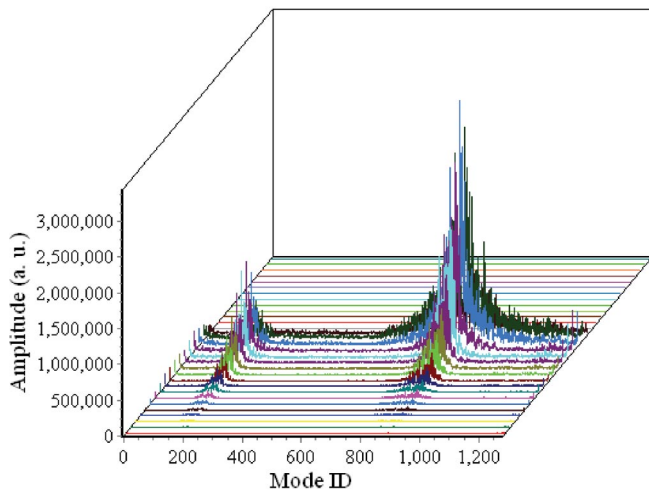


FIG. 5. (Color) Time evolution of horizontal unstable modes from mode 0 to 1279.

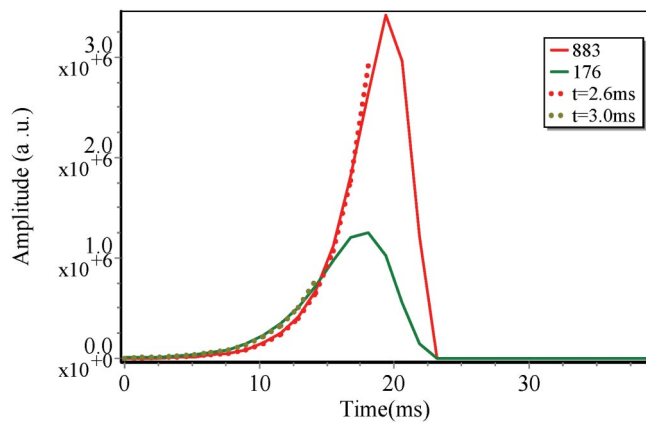


FIG. 6. (Color) Growth of two typical modes and their fitted results.

filling pattern was by 4, except for the gap for beam abort, the mode spectrum modes 0 to 1279 repeats, basically. We therefore use only from mode 0 to 1279 in our analysis, as shown in Fig. 5. By plotting the evolution of a mode and fitting it as exponential growth, we obtained the growth time of the mode. Figure 6 shows the growth of modes (883 and 176) and the fitted results. Because we use the block of 256 turns of data to get one amplitude, it contains systematic error to underestimate the growth rate for very fast growth. We have examined the analysis using the artificial inputs with given growth rates and modes. The analysis shown above shows complete agreements down to the growth time of 0.8 ms; below the value, the growth time saturates to 0.7 ms. Because the growth times of this experiment obtained with the analysis range over 0.9 ~ 8.9 ms and 0.8 ~ 3.3 ms for the horizontal and vertical planes, respectively, the systematic error in our case is negligible. For the analysis of a faster growth rate, we will need to use other methods [14].

### B. Unstable modes with a full field and without a solenoid field

Figures 7 show the unstable modes without a solenoid field for the horizontal and the vertical planes, respectively. The mode spectra at intervals of 128 turns are overlapped. Two groups of wide unstable modes appear both for the horizontal and the vertical planes; the higher group has the major contribution. The growth rates for both groups are almost the same. By changing the linear chromaticity, the spread of the modes seems to be affected; with smaller chromaticity, i.e., a faster growth rate, the spread becomes narrower. On the other hand, the peak positions of the modes are not affected.

When turning on the solenoids to full field, the unstable modes change drastically, as shown in Fig. 8 for the horizontal and vertical planes. Clearly, the unstable modes

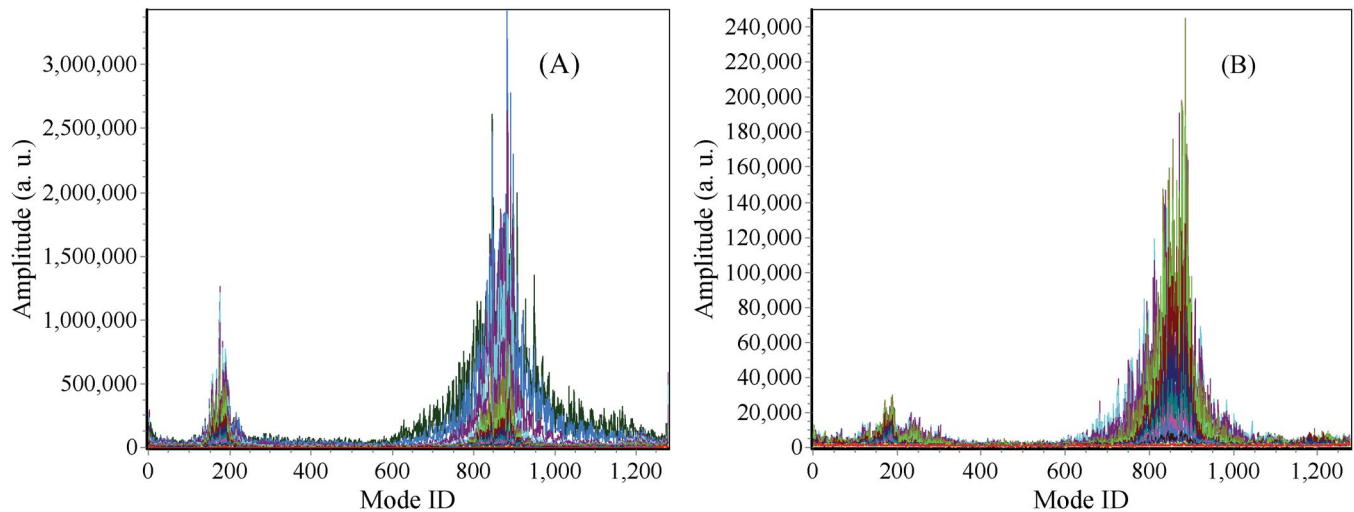


FIG. 7. (Color) Unstable modes without a solenoid field for the horizontal plane (a) and the vertical plane (b) [ $B_{sol} = 0%$ ,  $L_{sol} = 0%$ ].

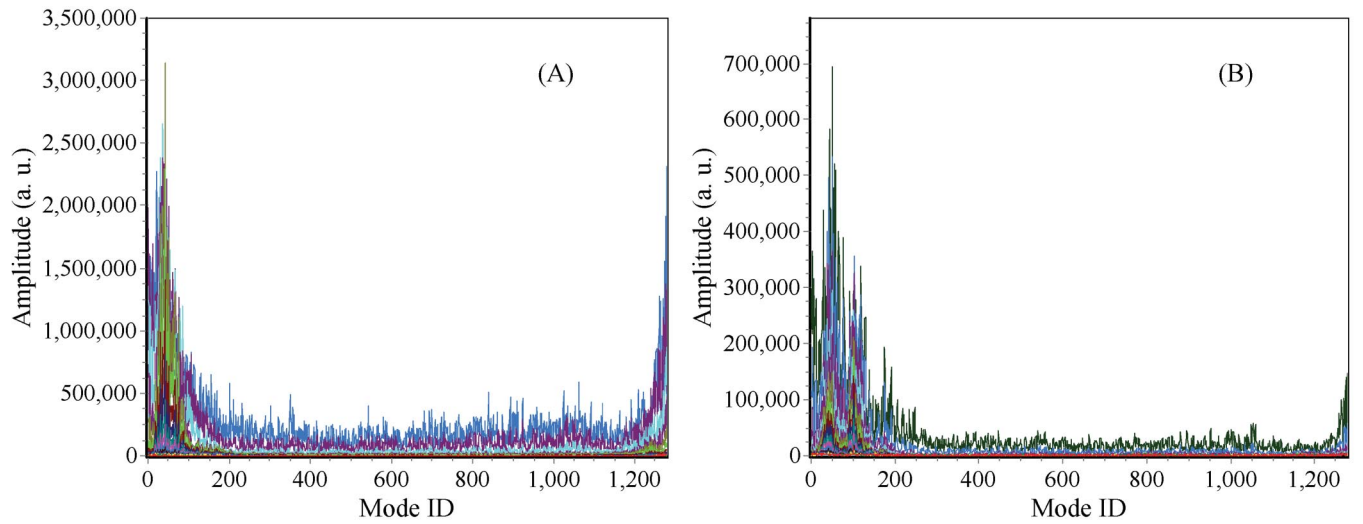


FIG. 8. (Color) Unstable modes with a full solenoid field for the horizontal plane (a) and the vertical plane (b) [ $B_{\text{sol}} = 100\%$ ,  $L_{\text{sol}} = 100\%$ ].

have been affected by the existence of the weak solenoid field both for the horizontal and the vertical planes. The result is completely consistent with the previous experiments [5,9]; with the solenoid field, the mode of the instability is governed by the circular motion of the electrons in the solenoid magnets.

### C. Effect of the strength of the solenoid

We changed the magnetic field of the solenoid from 100% to 20%, 10%, and 0% of the maximum field and measured the unstable modes. Figures 9 and 10 show the obtained unstable modes for 20% and 10%, respectively. Even with a very weak solenoid field, the unstable modes

show that the motion of the electron clouds were governed by the solenoid field, though the peak of the unstable modes were slightly moving to higher modes with lowering the solenoid field.

The growth rate of the instability is shown in Fig. 11. Note that we corrected the change of the growth rate due to a change of the linear chromaticity to the value corresponding to the full solenoid field, ( $\xi_x = 1.5$ ,  $\xi_y = 0.8$ ). The growth rates have offset  $-0.16 \text{ ms}^{-1}$ , both for the horizontal and vertical planes. Since the fitting error was estimated as around 5%, the scattering of the data corresponding the same  $B_{\text{sol}}$  are slightly larger than the error. This might be due to some uncorrected difference in experimental conditions.

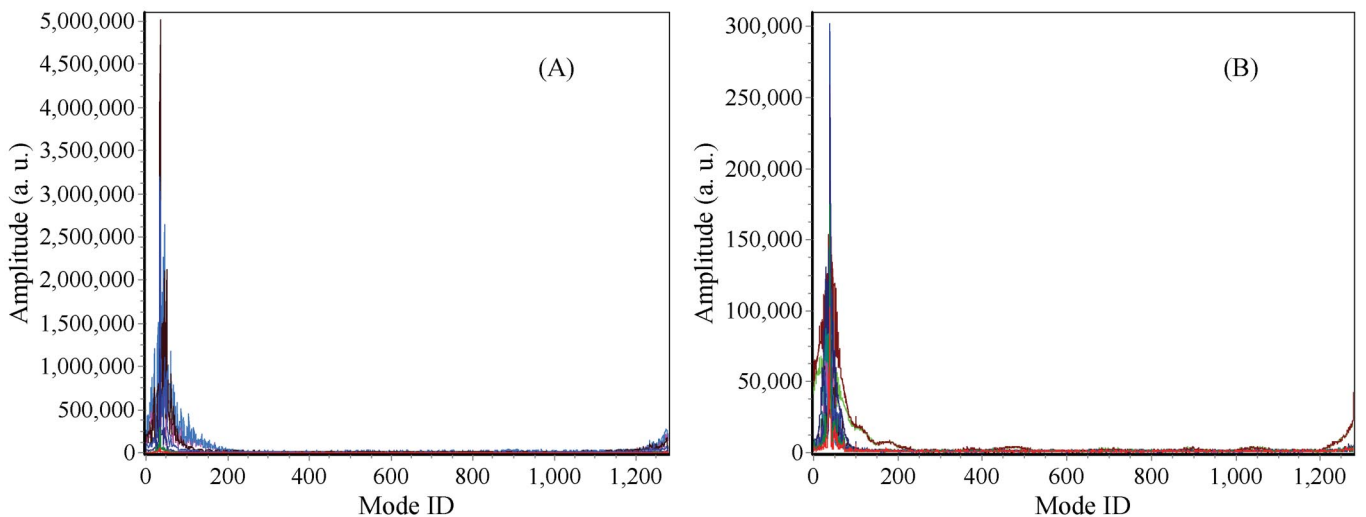


FIG. 9. (Color) Unstable modes with 20% of the solenoid field for the horizontal plane (a) and the vertical plane (b) [ $B_{\text{sol}} = 20\%$ ,  $L_{\text{sol}} = 100\%$ ].

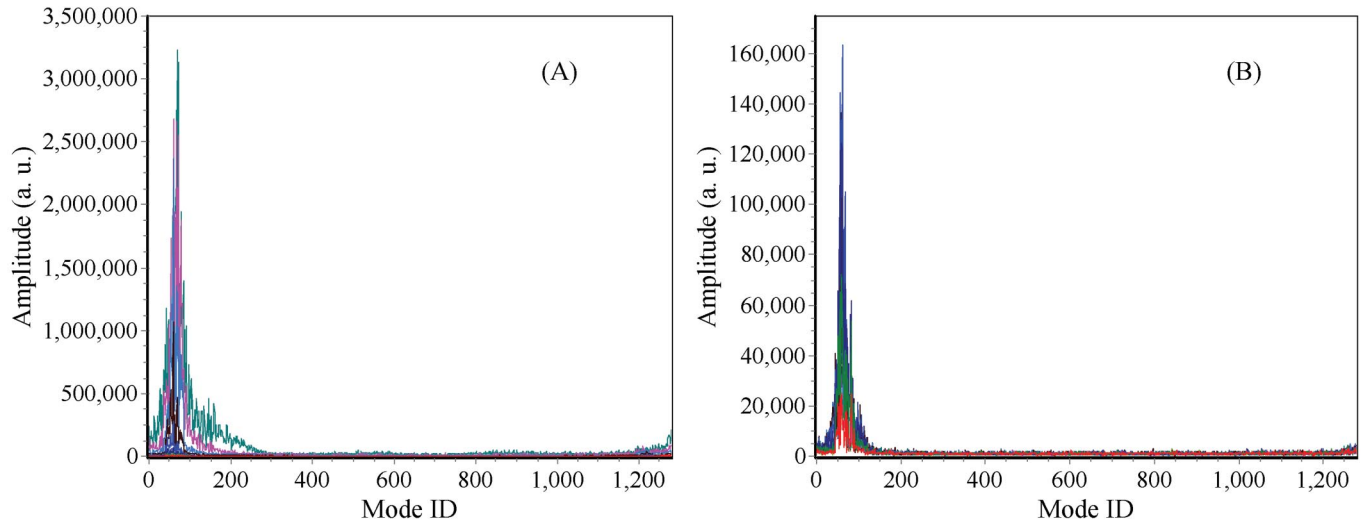


FIG. 10. (Color) Unstable modes with 10% of the solenoid field for the horizontal plane (a) and the vertical plane (b) [ $B_{\text{sol}} = 10\%$ ,  $L_{\text{sol}} = 100\%$ ].

Even with the scattering of the data, a large enhancement of the growth rate for both the horizontal and vertical planes are seen at lower solenoid fields. The growth rates with a full solenoid field are almost the same as the zero

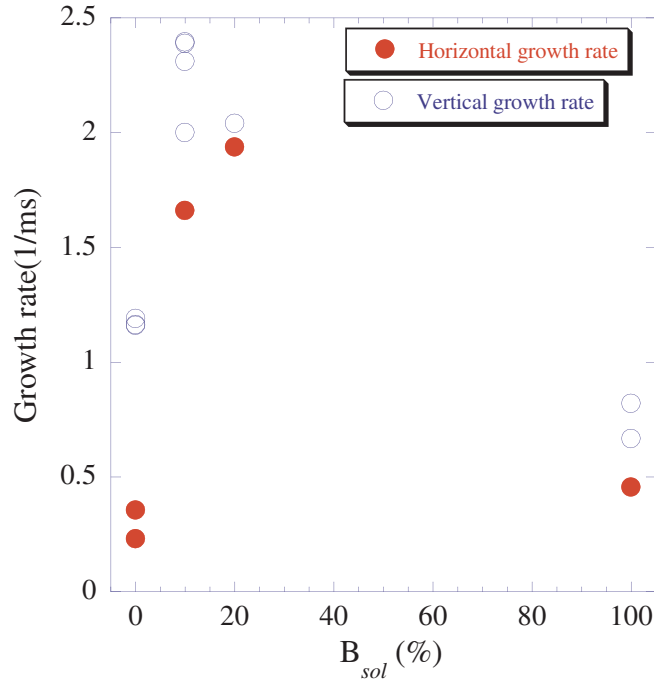


FIG. 11. (Color) Horizontal (solid circle) and vertical (open circle) growth rates of the instability with different  $B_{\text{sol}}$  settings. Note that points in the same  $B_{\text{sol}}$  correspond to the experimental result with different linear chromaticity. These growth rates are converted to those for  $\xi_x = 1.5$  and  $\xi_y = 0.8$  so that they have offset  $-0.16 \text{ ms}^{-1}$ , both for horizontal and vertical planes. The chromaticities ranged over  $1.08 \sim 9.36$  and  $0.8 \sim 9.64$  for the horizontal and vertical planes, respectively.

solenoid field for the horizontal plane, or slightly lower for the vertical plane.

#### D. Effect of the length of the solenoid

Next, we turned off 40% (east and west arc) or 20% (east arc) of the solenoid magnets in the ring while restoring the field strength of the rest of the magnets to the nominal ones. Under this condition, we expected two unstable modes, i.e., lower modes from the clouds in the solenoid field (around 20) and higher modes (around 180 and 880) from the cloud in the field-free regions. Figures 12 and 13 show the unstable modes with  $L_{\text{sol}} = 60\%$  and  $L_{\text{sol}} = 80\%$ , respectively. For the  $L_{\text{sol}} = 60\%$  case, two groups of modes both for the horizontal and vertical planes appear. Though the higher modes ( $\sim 150$ ) are slightly smaller than the modes without solenoids ( $\sim 180$ ), the lower modes ( $\sim 50$ ) are similar to those with a solenoid field of 100%. The growth rate of the upper modes is faster than the lower ones, as shown in Fig. 14. No clear difference from  $L_{\text{sol}} = 100\%$  is found in  $L_{\text{sol}} = 80\%$  case in both the horizontal and vertical plane.

The growth rate of the instability with  $L_{\text{sol}} = 60\%$  and  $L_{\text{sol}} = 80\%$  was similar to, or slightly smaller, than that with  $L_{\text{sol}} = 100\%$  as shown in Fig. 15.

## IV. COMPARISON WITH SIMULATION

A numerical study of the coupled-bunch instability caused by an electron cloud was made for a similar bunch-filling pattern for the KEKB LER [15]. The instabilities caused by the electron cloud in the simple drift-space without a magnetic field, the drift-space with a solenoid field (1 ~ 3 mT), and a strong dipole magnetic field of bending magnets were simulated. The spectra of the unstable modes are shown in Table III.

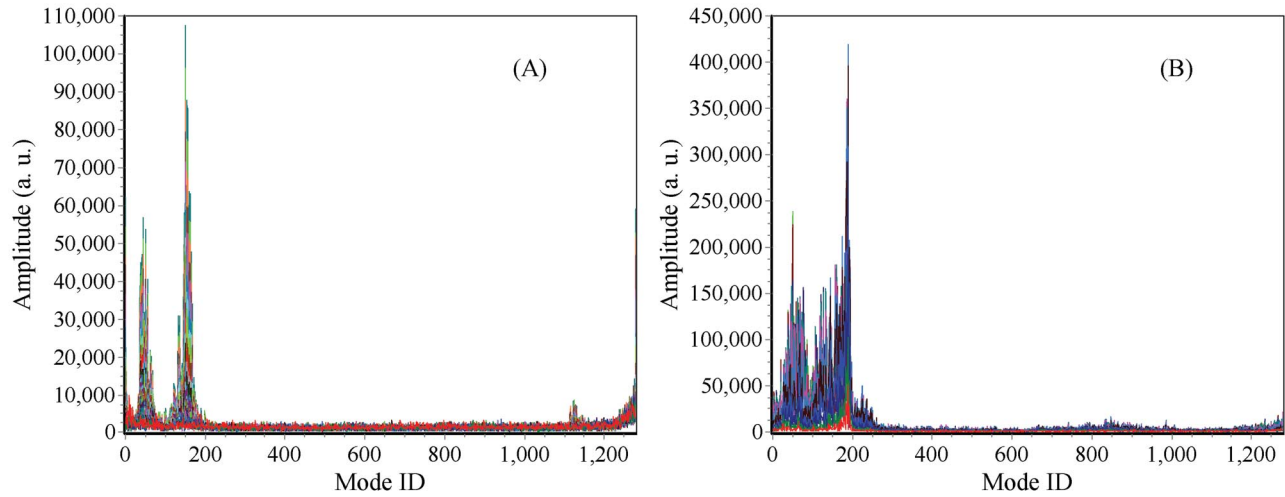


FIG. 12. (Color) Unstable modes with 40% of the solenoid magnets turned off for the horizontal plane (a) and the vertical plane (b) [ $B_{sol} = 100\%$ ,  $L_{sol} = 60\%$ ].

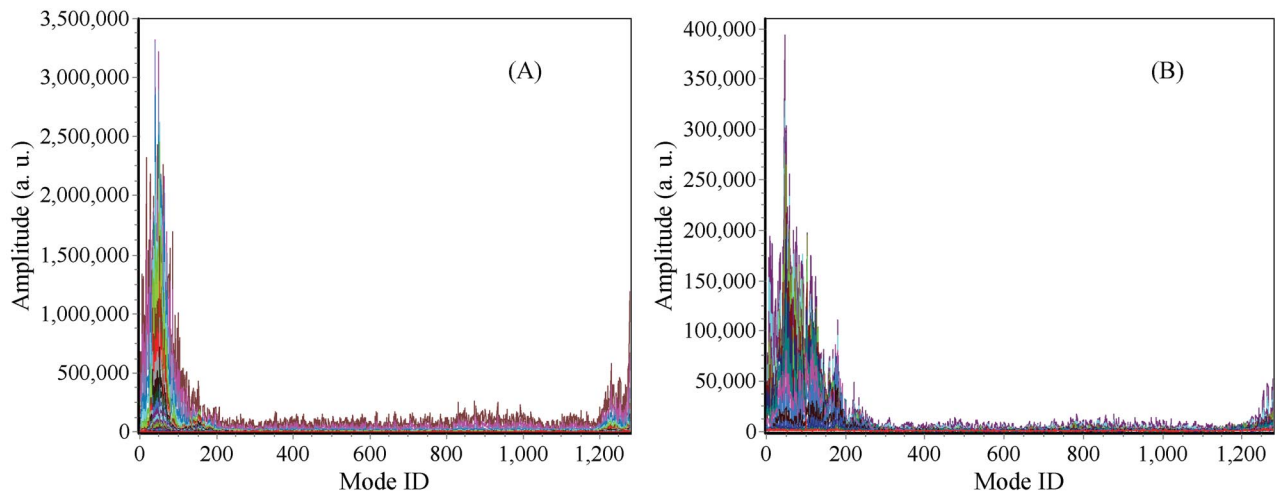


FIG. 13. (Color) Unstable modes with 20% of the solenoid magnets turned off for the horizontal plane (a) and the vertical plane (b) [ $B_{sol} = 100\%$ ,  $L_{sol} = 80\%$ ].

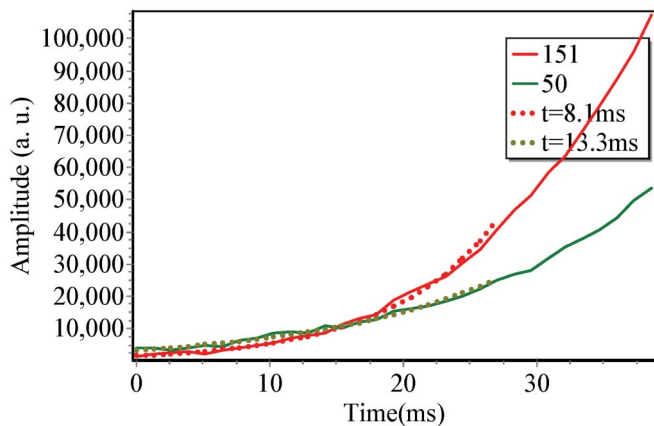


FIG. 14. (Color) Growth of lower and higher modes with the  $L_{sol} = 60\%$  case on the horizontal plane.

Figure 16 shows a summary of unstable modes obtained by this experiment for different solenoid fields. The upper modes than the red line, that is  $-45$  (horizontal) and  $-43$  (vertical), show that the phase of the oscillation advances with the longitudinal bunch position, such that the source of the instability is a focusing wake. On the other hand, the modes lower than the red line show that the phase of the oscillation delays with the bunch location, so that the source of the instability is a defocusing wake.

The experiment without a solenoid field supports the simulation where the electrons are almost uniformly emitted from the chamber wall, and the secondary emission rate is small ( $\delta_{2,max} = 1.0$ ) for both the horizontal and vertical cases.

The behavior of unstable modes when we changed the solenoid field showed good agreement with the simula-

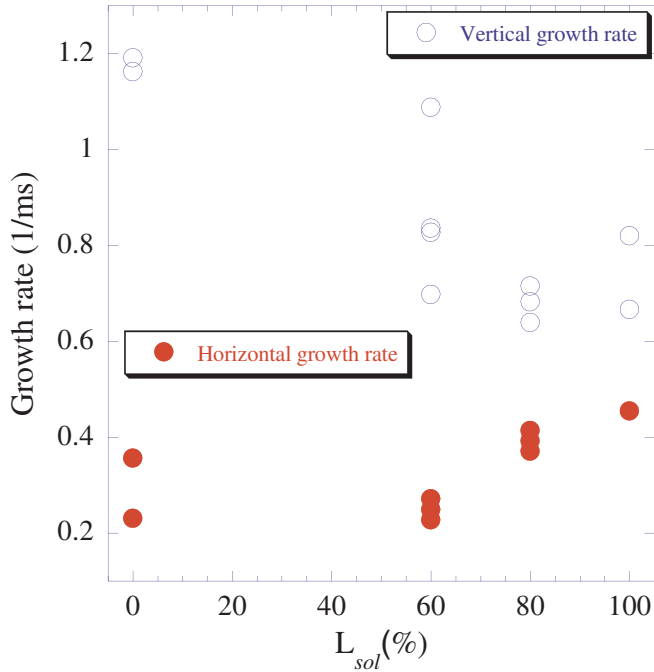


FIG. 15. (Color) Horizontal (solid circle) and vertical (open circle) growth rates of the instability with different  $L_{sol}$ . The chromaticities ranged over 0.797 ~ 3.06 and 1.4 ~ 3.3 for the horizontal and vertical planes, respectively.

tions. The tendency where the mode number increased with lowering the magnetic field also agreed between the experiment and the simulation.

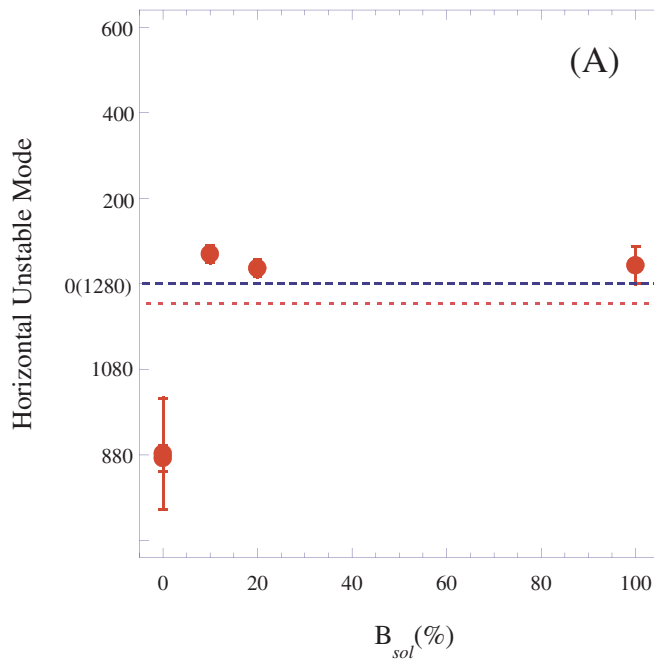


TABLE III. Simulated unstable modes, where  $\delta_{2,max}$  means the secondary emission rate. All the simulations except the larger  $\delta_{2,max}$  are using  $\delta_{2,max} = 1.0$ .

Cases	Horizontal	Vertical
Drift space w/o solenoid		
$e^-$ from Hit point by SR	180	840
Uniform emission	840	840
Larger $\delta_{2,max}(1.5)$	840 and 1100	840 and 1100
Weak solenoid field		
1 mT	20	10
2 mT and 3 mT	$\sim 0$	$\sim 0$
Bending magnet	1234	160 and 840

In the simulation, the growth rate of the instabilities strongly depends on the secondary yield of the photoelectron ( $\delta_{2,max}$ ) without the solenoid field. With the solenoid field, the wake field of the instability is governed by the motion of photoelectrons near the chamber wall [15]. Figure 17 shows the simulated growth rate of the vertical instability with the strength of the field of the solenoid, with  $\delta_{2,max} = 1.5$  and  $\delta_{2,max} = 1.0$ . Again the experimental result supports the simulation with lower  $\delta_{2,max}$ . A more detailed study for both the simulation and the experiment will be needed to explore the remaining difference between them.

In the case of shorter area covered by a solenoid field, the main unstable modes seem to be affected by the unstable mode coming from the solenoid field. It might be

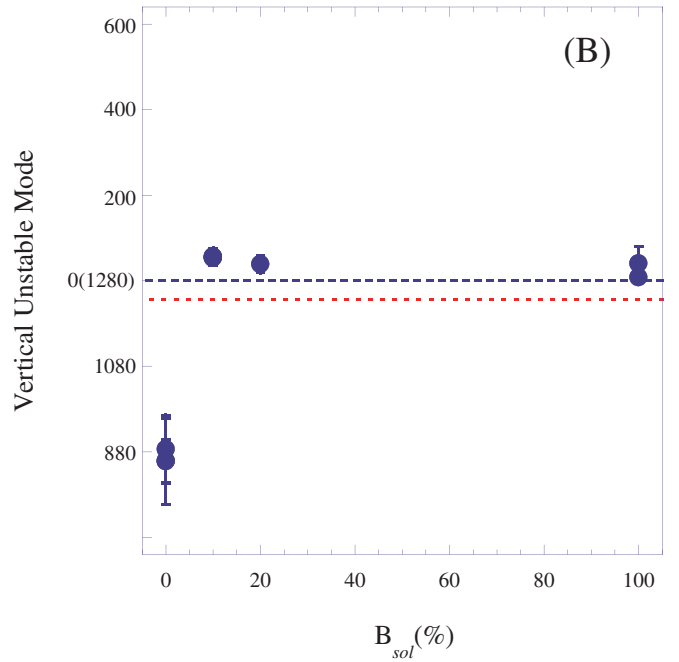


FIG. 16. (Color) Unstable modes [horizontal (a); vertical (b)] with a solenoid field. The error bars reflect the bottom-to-bottom width of the unstable modes. The red dotted line show the integer part of the betatron tune. The upper modes than those of the red line are caused by the focusing wake and the lower modes are caused by the defocusing wake.



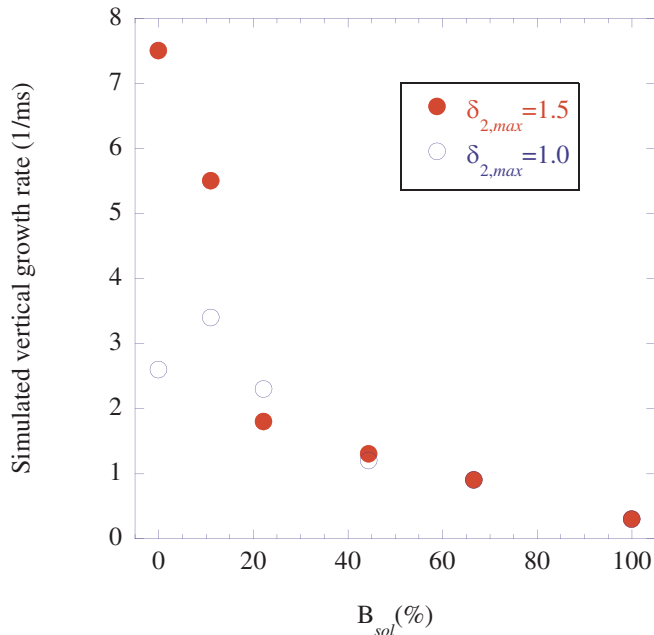


FIG. 17. (Color) Simulated vertical growth rate for the case of  $\delta_{2,max} = 1.5$  (solid circle) and  $\delta_{2,max} = 1.0$  (open circle), where  $\delta_{2,max}$  is the secondary yield of the photoelectron.

regarded as some kind of mixture of unstable modes of the lower drift  $\sim 200$  mode and the solenoid mode  $\sim 50$  as very near modes, though there are no  $\sim 800$  modes that are strongest on the drift mode.

## V. CONCLUSION

We measured the unstable modes of the coupled-bunch instability caused by electron clouds. We observed the drastic change of the mode spectra, the retarded mode to advanced mode, for switching on to off of the solenoid magnets. The behavior is clear evidence of an electron cloud induced coupled-bunch instability. Both in the horizontal and vertical planes, the experimental results support the simulation where the instability is dominated by the electron clouds in the drift space with the lower secondary emission rate  $\delta_{2,max} = 1.0$  rather than 1.5. The mode spectrum shows that the ring is almost covered by the solenoid magnet, and the electron cloud in the drift space and in the bending magnet is not dominant now for the coupled-bunch instability. The mode spectra for the solenoid magnets show a higher frequency than those given by the simulation. The difference suggest that the effective field strength is weaker ( $\sim 1$  mT) than our expectation; otherwise, electrons may stay nearer to the beam position than the chamber surface. The possibility of such a weaker field strength is, however, low. The behavior of the growth rate with changing a solenoid field also supported the simulation with lower  $\delta_{2,max}$ . The modes appeared with a shorter area covered by solenoid is complicated and further simulation study will be needed.

## ACKNOWLEDGMENTS

The authors would like to acknowledge members of the KEKB commissioning group for their help during our experiments.

- [1] M. Izawa, Y. Sato, and T. Toyomasu, Phys. Rev. Lett. **74**, 5044 (1995).
- [2] K. Ohmi, Phys. Rev. Lett. **75**, 1526 (1995).
- [3] T. Holmquist and J. Rogers, Phys. Rev. Lett. **79**, 3186 (1997).
- [4] Z. Guo, H. Huang, S. P. Li, D. K. Liu, L. Ma, Q. Qin, J. Q. Wang, S. H. Wang, G. Xu, C. Zhang, Z. Zhao, Y. H. Chin, H. Fukuma, S. Hiramatsu, M. Izawa, T. Kasuga, E. Kikutani, Y. Kobayashi, S. Kurokawa, K. Ohmi, Y. Sato, Y. Suetsugu, M. Tobiyama, K. Tsukamoto, K. Yokoya, and X. L. Zhang, Phys. Rev. ST Accel. Beams **5**, 124403 (2002).
- [5] Su Su Win, Hitoshi Fukuma, Kazuito Ohmi, and Shin-ichi Kurokawa in *Proceedings of ECLLOUD'02* (CERN Report No. CERN-2002-001), p. 199.
- [6] M. Arinaga, J. Flanagan, S. Hiramatsu, T. Ieiri, H. Ikeda, H. Ishii, E. Kikutani, T. Mimashi, T. Mitsuhashi, H. Mizuno, K. Mori, M. Tejima, and M. Tobiyama, Nucl. Instrum. Methods Phys. Res., Sect. A **499**, 100 (2003).
- [7] Y. Funakoshi, K. Akai, K. Ebihara, K. Egawa, A. Enomoto, J. Flanagan, H. Fukuma, K. Furukawa, T. Furuya, J. Haba, S. Hiramatsu, T. Ieiri, N. Iida, H. Ikeda, T. Kageyama, S. Kamada, T. Kamitani, S. Kato, M. Kikuchi, E. Kikutani, H. Koiso, M. Masuzawa, T. Mimashi, A. Morita, T. Nakamura, H. Nakayama, Y. Ogawa, K. Ohmi, Y. Ohnishi, N. Ohuchi, K. Oide, M. Shimada, S. Stanic, M. Suetake, Y. Suetsugu, T. Sugimura, T. Suwada, M. Tawada, M. Tejima, M. Tobiyama, S. Uehara, S. Uno, S. Win, N. Yamamoto, Y. Yamamoto, Y. Yano, K. Yokoyama, M. Yoshida, M. Yoshida, S. Yoshimoto, and F. Zimmermann, in *Proceedings of the Particle Accelerator Conference, Knoxville, TN, 2005* (IEEE, Piscataway, NJ, 2005).
- [8] M. Tobiyama and E. Kikutani, Phys. Rev. ST Accel. Beams **3**, 012801 (2000).
- [9] M. Tobiyama, J. W. Flanagan, H. Fukuma, S. Kurokawa, K. Ohmi, and S. S. Win, in *Proceedings of the Particle Accelerator Conference, Knoxville, TN, 2005* (Ref. [7]).
- [10] J. D. Fox, R. Larsen, S. Prabhakar, D. Teytelman, A. Young, A. Drago, M. Serio, W. Barry, and G. Stover, in *Proceedings of the 1999 Particle Accelerator Conference, New York* (IEEE, Piscataway, NJ, 1999), p. 636.
- [11] S. Prabhakar, J. D. Fox, D. Teytelman, and A. Young, Phys. Rev. ST Accel. Beams **2**, 084401 (1999).
- [12] D. Teytelman, J. Fox, S. Prabhakar, and J. M. Byrd, Phys. Rev. ST Accel. Beams **4**, 112801 (2001).
- [13] S. Heifets and D. Teytelman, Phys. Rev. ST Accel. Beams **8**, 064402 (2005).
- [14] D. Teytelman, Ph.D. thesis, Stanford University (Report No. SLAC-R-633, 2003).
- [15] S. S. Win, K. Ohmi, H. Fukuma, M. Tobiyama, J. Flanagan, and S. Kurokawa, Phys. Rev. ST Accel. Beams **8**, 094401 (2005).